# Numerical Modelling of Ground Heat Exchangers with Different Ground Loop Configurations for Direct Geothermal Applications

## Modélisation numérique des échangeurs de chaleur souterrains avec différentes configurations de boucles pour les applications géothermiques directs

Bidarmaghz A., Narsilio G., Johnston I.
*Department of Infrastructure Engineering, The University of Melbourne, Australia*

ABSTRACT: The design of ground heat exchangers (GHEs) involves the selection of detailed configuration options. However, there is limited understanding of the relative importance of different design choices on performance. This study investigates the effects of different design parameters such as pipe configuration and fluid flow rate on the heat extraction rate, and will be helpful to design a system which is energy efficient and cost effective. Different pipe configurations in vertical grouted boreholes including single U-pipe, double U-pipe, and double cross U-pipes for small diameter boreholes, and spiral and multiple U-pipes for larger diameter boreholes, are modelled in detail using state-of-the-art finite element methods. The effects of GHE configurations and fluid flow rate on system efficiency is determined and contrasted. Numerical results indicate that the thermal performance of the system is enhanced by transitioning from laminar to turbulent regime, and by increasing the volume of carrier fluid inside the pipes for a given GHE length (i.e., single versus double pipes). However, in larger diameter boreholes, GHE's thermal performance does not change significantly for different pipe configurations with similar pipe lengths inside the borehole (i.e., spiral versus multiple U-pipes).

RÉSUMÉ : La conception des échangeurs de chaleur souterrains (ECS) nécessite un choix parmi différentes configurations. Cependant, la compréhension de l'importance relative des différents choix de conception sur les performances est limitée. Cette étude examine les effets des différents paramètres de conception, tels que la configuration des tuyaux ou encore le débit du fluide sur le taux d'extraction de la chaleur. Elle sera utile pour concevoir un système éco-énergétique et rentable. Différentes configurations de tuyauterie dans des forages verticaux injectés, y compris le simple U-tube, le double U-tube et le U-tube en double croix pour forages de petit diamètre, et de multiples spirales et U-tuyaux pour forages de grand diamètre, sont modélisés en détail en utilisant des méthodes aux éléments finis. Les effets de la configuration d'un ECS et le débit du fluide sur l'efficacité des systèmes sont déterminés et comparés. Les résultats numériques indiquent que le rendement thermique est accru par la transition du régime laminaire au régime turbulent, et en augmentant le volume de fluide porteur à l'intérieur des tubes d'ECS d'une longueur donnée. Toutefois, dans les puits de grand diamètre, la performance thermique d'un ECS ne change pas de façon significative pour les configurations de tuyaux différents avec des longueurs de tuyaux semblables à l'intérieur du puits (par exemple, en spirale ou multiples U-tubes).

KEYWORDS : Direct Geothermal Energy, Vertical Ground Heat Exchangers, Ground Loop Configurations, Numerical Modelling

## 1 INTRODUCTION

In recent years, geothermal energy has become an alternative energy source with great environmental and economical benefits. Geothermal energy sources range from shallow depths to hot water and hot rocks a few kilometers below the ground surface. Ground source heat pump (GSHP) systems use shallow geothermal energy sources for heating, cooling or even hot water supply of commercial, industrial and residential buildings. The ground temperature below about 5 to 10 meters depth is nearly constant over the year and is close to the mean ambient temperature. Therefore, the ground is warmer than the atmosphere in winter and cooler in summer. GSHP technology takes advantage of this relatively constant ground temperature. In winter time, heat is extracted from the ground and transferred to the indoor area via GSHPs. This process is reversed in summer.

A critical part of GSHP systems is the ground heat exchanger (GHE), with vertical GHEs being a common choice due to their reduced footprint and significantly higher energy performance characteristics in comparison to horizontal systems due to smaller temperature fluctuations in the ground at depth (Banks 2008). The performance of GSHP systems depends on the amount of the heat transferred between the ground and the carrier fluid which circulates within the pipes embedded in the GHEs. Several design choices are required; however, only a relatively limited number of numerical, analytical and experimental studies have been conducted to assist in optimizing the design parameters.

Pipe loop configuration, fluid flow rate and pipe separation are some of many design parameters which affect system efficiency and they are numerically modelled here. Heat transfer and fluid flow are the two main physical processes combined in the numerical model. Heat exchange rates, which arise from temperature distributions in the ground, at the borehole wall and in the carrier fluid in different ground loop configurations, are discussed for a variety of ground loop configurations and operating conditions.

## 2 MODEL DESCRIPTION

A model of GHEs was developed from first principles, accounting for fluid flow and heat transfer through the various components of the GHE. The model represents GHEs that consist of grouted boreholes placed vertically in the ground, with water circulating within the pipes of these GHEs. Details of these models follow.

### 2.1 *3D finite element model*

The motion of the carrier fluid in the pipes is described by the well-known Navier-Stokes equations (NS). These equations are the formulation of the continuity law for an incompressible flow which represents the conservation of mass, and the formulation for conservation of momentum described in Eqs (1) and (2) respectively:

$$\rho\nabla.\mathbf{u} = 0 \tag{1}$$

$$\rho\frac{\partial\mathbf{u}}{\partial \mathrm{t}} + \rho(\mathbf{u}.\nabla)\mathbf{u} = \nabla.\left(-PI + \mu(\nabla\mathbf{u}) + (\nabla\mathbf{u}^T)\right) + F \tag{2}$$

where $\rho$ is the fluid density in kg/m$^3$, $\mathbf{u}$ represents the velocity field in m/s, $P$ is pressure in Pa, $I$ is the identity matrix, μ is the dynamic fluid viscosity in Pa.s, $T$ represents the absolute temperature in K, and $F$ is a volume force field of various origins (for example, gravity) expressed in N/m$^3$.

In a turbulent flow, all quantities in the previous equations fluctuate in time and space. The averaged representation of turbulent flow divides the flow quantities into an averaged value and a fluctuating part. The decomposition of the flow field into an average part and a fluctuating part, followed by insertion into the NS equations and then averaging, gives the Reynolds Average Navier Stokes equations (RANS), which allows a less expensive computational modelling of fluid flow in the turbulent regime, and is used herein:

$$\rho\frac{\partial\mathbf{u}}{\partial \mathrm{t}} + \rho\mathbf{u} + \nabla\mathbf{u} + \nabla.\overline{(\rho\boldsymbol{u}'\otimes\boldsymbol{u}')} = -\nabla P + \nabla.\mu(\nabla\mathbf{u} + (\nabla\mathbf{u})^T) + F \tag{3}$$

Heat transfer from the ground to the heat exchanger and the carrier fluid can be modelled using conduction and convection equations. This process is the result of the flow of energy due to temperature differences. The generalized governing equation for heat transfer can be expressed as:

$$\rho_m C_{p,m}\frac{\partial T}{\partial \mathrm{t}} + \rho_m C_{p,m}\mathbf{u}.\nabla T = \nabla.(k_m\nabla T) + Q \tag{4}$$

where $\rho_m$ is the density of a given medium (i.e., fluid or solid) in kg/m$^3$, $\mathbf{u}$ is the velocity field in m/s, $k_m$ represents the thermal conductivity of the given medium (i.e., fluid or solid) in W/(mK), $C_{p,m}$ represents the heat capacity of the medium (i.e., fluid or solid) in J/(kgK), and Q is an external heat source in W/m$^3$. Note that "solid" can refer to soil, rock, concrete, grout, steel or any other solid forming part of the subsurface components of the GHEs.

Heat transfer in the carrier fluid circulating in the pipes results from a combination of heat conduction and convection and can be modelled using Eq (4) in full. Here the fluid velocity field $\mathbf{u}$ is coupled to Eqs (1) and (2). In other words, the velocity field $\mathbf{u}$, found by solving the governing Eqs (1) and (2), is used in Eq (4) when modelling the heat transfer by conduction and convection within the pipes.

On the other hand, heat transfer in solids, which occurs in the ground, in the borehole and in the pipe wall, also uses Eq (4), however, the second term of the left hand side vanishes as the velocity field is null (i.e., no fluid flow), thus Eq (4) reduces to a conduction only phenomenon. This is valid in the absence of groundwater flow.

#### 2.1.1 *Numerical modelling of small diameter GHEs with single, double and double cross U-pipes*

The numerical models consist of 30 m long cylindrical vertical GHEs, 0.14 m in diameter, comprising high density polyethylene (HDPE) pipes embedded in grout, with assumed constant thermal properties (see Table 1 for details).

Table 1. GHEs' material thermal properties.

| Material | Thermal conductivity [W/(mK)] | Heat capacity [J/(kgK)] |
|---|---|---|
| Soil/Rock | 2 | 1300 |
| Grout | 2 | 854 |
| Water | 0.6 | 4200 |
| HDPE pipes | 0.45 | - |

A single, double or double cross HDPE U-pipe GHE with a pipe diameter of 0.025 m and wall thickness of 0.003 m is sequentially modelled to assess the thermal response of these different pipe configurations. The pipe separation (i.e., distance between inlet and outlet pipes) is set at its maximum value; in the other words, pipes are placed as close as possible to the borehole wall. This is known to render higher thermal efficiency than more closely spaced pipe placements and is common installation practice. The pipe cover, C, is kept equal in all cases modelled here (i.e., $C_1$ = $C_2$ = $C_3$). Therefore, the GHEs embedding single and double cross U-pipes have the same pipe separation $S_1 = S_2 = 0.11$ m, but due to geometry limitations, the pipe separation reduces to $S_3 = 0.07$ m in double U-pipe settings (see Figure 1). A soil cylinder with a diameter of 7 m surrounding the GHE completes the FEM model.

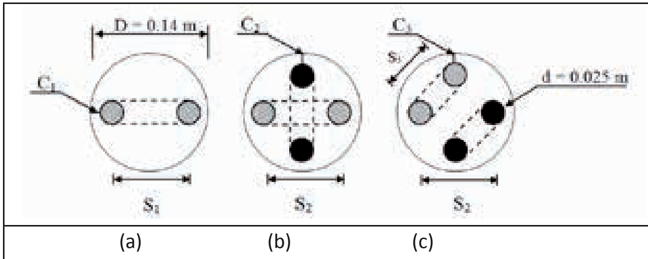


Figure 1. GHE pipe configurations: (a) single U-pipe, (b) double cross U-pipe, (c) double U-pipe.

A 5-day transient study with prescribed fluid flow rates varying from laminar to turbulent regime is conducted on these different GHE configurations. The recommended FEM mesh pattern consists of elements with higher mesh density near and in the pipes, becoming coarser in the radial direction, away from the center of the GHE and towards the ground. Figure 2 shows an example of a 3D model configuration and FEM mesh pattern for a GHE with two U-pipes.

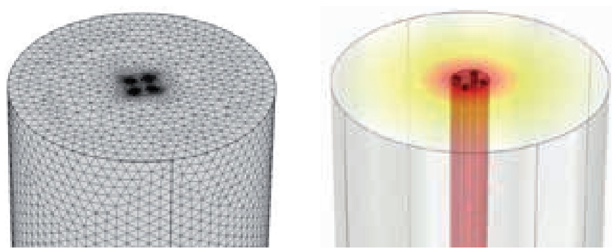

(a) (b)

Figure 2. Example of a 3D FEM model section: (a) FEM mesh of a GHE with two U-pipes; (b) detail of temperature distribution.

#### 2.1.2 *Numerical modelling of large diameter GHEs with spiral pipes and multiple U-pipes*

The numerical models consist of 30 m long cylindrical vertical GHEs, 0.46 m in diameter, comprising spiral and straight HDPE pipes embedded in grout. The GHE is surrounded by a soil cylinder of 7 m diameter.

A larger borehole diameter will be typically (but not always) required when HDPE pipes are used in a spiral configuration due to the stiffness of the pipe. GHEs with spiral pipes and with single, double or triple U-pipes are modelled for comparision.

HDPE pipes are 0.025 m in diameter and with a 0.003 m wall thickness. The spiral configuration consists of an inlet pipe with a 0.3 m spiral major diameter and axial pitches which are varied, sequentially, between 0.2 m to 1 m; and a straight outlet pipe (Figure 3-a). Consequently, different pipe lengths are modelled to investigate the effects on heat extraction rate. Numerical results obtained from the above modelling are compared to the results from 0.46 m diameter, 30 m long GHEs with single, double and triple U-pipes, 0.025 m in diameter embedded within, which render the same pipe lengths as the ones in the spiral configurations (see Figure 3-b through -d). The same assumed constant material properties are shown in Table 1. The FEM mesh in these model follows the same mesh density distribution as shown in Figure 2.

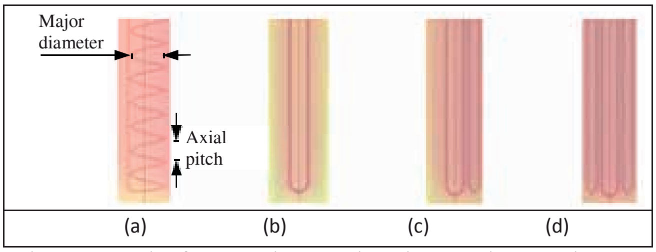


Figure 3. Detail of GHEs with (a) spiral pipe, (b) single U-pipe; (c) double U-pipe, (d) triple U-pipe.

### 2.2 *Initial and boundary conditions*

A depth dependent temperature, varying between 8.7°C at the ground surface and 18.6°C for the first 10 m below the ground surface, is applied over the entire model (the GHEs and the ground) as initial and far-field boundary condition. Below this relatively thin layer and from about 10 m to 30 m below the ground surface, a constant temperature of 18.6°C is applied to the rest of the model. To account for the thermal interaction between conductive and convective heat transfer, the inlet temperature and fluid flow rate are also specified as boundary conditions. The simulations are run in heating mode, that is, whilst extracting heat from the ground. For simplicity, a typical inlet temperature of 5ºC is prescribed in the inlet pipe(s) of the modelled GHEs. For the fluid flow simulation inside the pipes, a no slip boundary condition is applied on the pipe walls, in other words, the water velocity on the pipe wall is set to zero; and a reference atmospheric pressure is set in the outlet pipe(s) for the purpose of forced convection.

## 3 RESULTS

In this section a brief summary of the model validation is presented together with the results of the numerical simulations of the various ground loop configurations and fluid flow rates.

### 3.1 *Model validation*

Numerical results obtained from the transient study of GHE with a single U-pipe were validated against analytical solutions that are based on Infinite Line Source Model (ILSM), Finite Line Source Model (FLSM) and Cylindrical Source Model (CSM). Details of these solutions can be found elsewhere (Bernier 2001, Deerman 1990, Jun *et al.* 2009, Lamarche and Beauchamp 2007, Marcotte and Pasquier 2008). As an example, Table 2 summarises the results in terms of heat extraction rate q and outlet pipe(s) temperature $T_{out}$ for the case of a 30 m long GHE, with 0.025 m diameter single U-pipe and water flow rate of ~14.5 l/min after 120 hrs of operation. Numerical results are in good agreement with the FLSM, which is the most reliable model among the previously mentioned models. The numerical results are also within the range of measurements reported for full scale experiments (Banks 2008, Gao *et al.* 2008, Hamada *et al.* 2007, Miyara *et al.* 2011).

Table 2 Comparison between analytical and numerical solutions.

| Parameter | ILSM | FLSM | CSM | Field data | This work |
|---|---|---|---|---|---|
| q [W/m] | 30.67 | 44.93 | 32.14 | 10-60 | 48.87 |
| $T_{out}$ [°C] | 5.93 | 6.36 | 5.97 | - | 6.48 |

### 3.2 *Numerical results and discussion*

With the numerical model validated for the single U-pipe case, other GHE pipe configurations were then examined: the double U-pipe and the double cross U-pipe. Cross sections of all small diameter GHEs were shown in Figure 1. We studied the effects on the thermal performance of these GHE configurations caused by variations of water flow rate. Figure 4 shows a summary of the numerical results for GHEs with single, double and double cross U-pipes, expressed as the total average heat extraction of each GHE per meter depth of borehole.

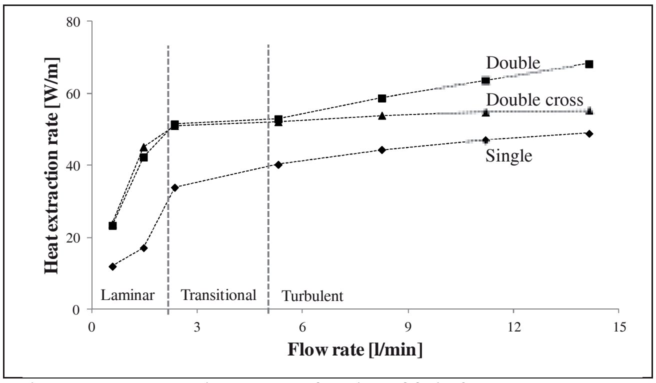


Figure 4. Heat extraction rate as a function of fluid flow rate.

As the average water flow rate increases in the pipe, heat extraction rate first tends to increase at a high rate for all GHE configurations considered here. However, above a flow rate of approximately 5.30 l/min (u = 0.18 m/s) the flow becomes turbulent and the increase in the heat extraction rate with flow (or Reynolds number) slows down in comparison with the laminar regime. Thus higher flow rates, do not necessarily results in significant increase in system's efficiency and the rate of increase declines with Reynolds number beyond a certain threshold. The addition of a second U-pipe to a single U-pipe configuration does not double the thermal performance but achieves between about 40% to 90% additional performance, depending on the volume of the water in contact with the ground heat source/sink. Nevertheless, savings may be achieved in terms of drillings costs, given the reduction in the total number or length of GHEs than would be needed with a single U-pipe. The comparison of double U-pipe and double cross U-pipe configurations shows that GHEs with double U-pipe perform about up to 23% better while the water fluid flow is in turbulent regime, and has nearly the same performance in laminar regime, for the pipe separations studied here.

For the case of large diameter GHEs, Figure 5 shows the effect of axial pitch in GHEs with spiral pipes. The figure shows that smaller axial pitches, which render longer pipe length, result in higher thermal performance since there is larger contact area between the water and the ground heat source/sink.

Comparing the thermal performance between large diameter GHEs with spiral pipes and U-pipes, Table 3 shows that for a given total water flow rate of 14.5 l/min in each GHE, and borehole length and diameter, GHEs with same pipe length embedded within have nearly the same thermal performance regardless of pipe geometry specifically when dealing with more than one U-pipe (i.e., spiral and multiple U-pipes with 0.14 m of pipe separation). Therefore, GHEs with multiple U-pipes instead of spiral pipes would be recommended, since (i) installation of GHEs with spiral pipes is, in general, not as easy to implement as with U-pipes due to HDPE pipe stiffness, and (ii) they have nearly the same thermal performance. In these large diameter GHEs, a relatively minor change in heat extraction rate is suggested by the numerical results when the total the flow rate through the GHE is increased. The rightmost column in Table 3 summarises the numerical results of doubling and tripling the flow rates in GHE with double U-pipes and triple U-pipes respectively (the same fluid flow rate is applied to each U-loop of the GHEs).

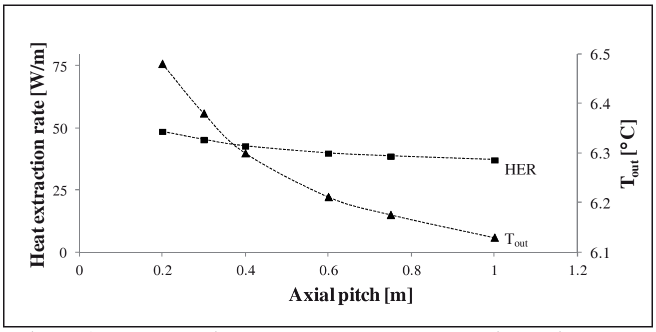


Figure 5. Heat extraction rate and outlet temperature in a spiral GHE with different axial pitches.

Table 3. Comparison of spiral and U-pipes GHE thermal performance for varying pipe lengths.

| Geometry | Axial Pitch [m] | Pipe length [m] | Flow rate of 14.5 l/min in each GHE | Flow rate of 14.5 l/min in each U-pipe |
|---|---|---|---|---|
| | | | Heat extraction rate [W/m] | Heat extraction rate [W/m] |
| Spiral 1 | 0.2 | 180 | 48.63 | 48.63 |
| Triple U | - | 180 | 49.71 | 51.15 |
| Spiral 2 | 0.3 | 120 | 45.35 | 45.35 |
| Double U | - | 120 | 44.07 | 45.10 |
| Spiral 3 | 1 | 60 | 37.13 | 37.13 |
| Single U-pipe | - | 60 | 32.53 | 32.53 |

The previous observations will not vary significantly if different pipe separations in the U-pipes are used. To investigate the effects of pipe separation on GHEs thermal performance, single, double and triple U-pipes with different inlet-outlet pipe separations were simulated. Figure 6 shows variations of pipe separation for multiple U-pipe GHEs and how this affects the heat extraction rate. Pipe separation variations between $S_S$ = 0.04 m and $S_L$ = 0.28 m for the 0.46 m diameter GHE result in heat extraction rate increasing about 7% to 23%.

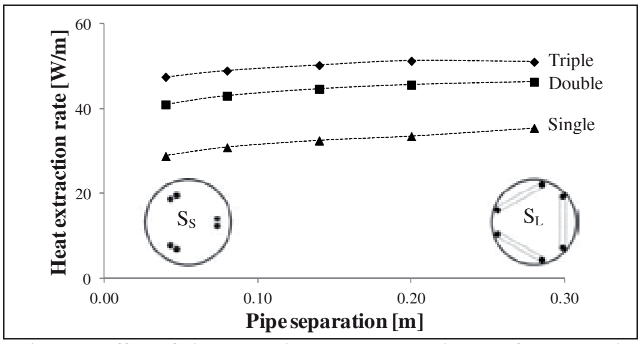


Figure 6. Effect of pipe separation on heat extraction rate for GHEs with single, double and triple u-pipes.

It is worth mentioning that pipe separation has a stronger influence on GHEs with single U-pipe than that of a triple U-pipe, the reason being that in multiple U-pipes, increasing the separation reduces the thermal interference between inlet and outlet pipe of one U-pipe but at the same time increases mutual interference between different U-pipes inside the GHE.

## 4 CONCLUSIONS

The outcomes of the multiple simulations performed in this work show that GHE configuration may affect system efficiency. Based on numerical results in a large diameter borehole and for a given borehole length, it seems that as long as the same pipe length is embedded inside the borehole, thermal performance of the system is not significantly related to pipe geometry placement, at least for the spiral and multiple U-pipes analysed here. However, comparison of small diameter GHEs with double and double cross U-pipe shows between 8% to 23% better performance of the former one. Nevertheless, the addition of a second U-pipe to both small and large diameter GHEs achieves significant (40-90%) additional thermal performance and could lead to important cost savings when compared with single pipe systems due to reduced drilling costs.

Heat extraction rates tend to increase rapidly as the Reynolds number increases in the laminar regime; however, the rate of increase reduces with Reynolds numbers once the flow becomes turbulent. This indicates that when considering the size of the fluid circulating pump and its operational cost, highly turbulent fluid flow will not necessarily result in a more efficient system overall. Regardless of number of U-pipes inside the GHE, larger pipe separation improves the system efficiency. However, as the number of U-pipes in the GHE increases, this effect becomes less pronounced due to thermal interference occurring between different U-pipes.

## 5 ACKNOWLEDGEMENTS

This work is partially supported by funding of $1.6 M from the Victorian Government's Energy Technology Innovation Strategy (ETIS) Pilot Demonstration Program (SEPD) and The University of Melbourne's Research Collaboration Grant.

## 6 REFERENCES

Banks, D. 2008. An introduction to thermogeology: ground source heating and cooling, Wiley-Blackwell.

Bernier, M.A. 2001. Ground-coupled heat pump system simulation. *ASHRAE Transactions* 107, 605-616.

Deerman, J. 1990. Simulation of vertical U-tube ground-coupled heat pump systems using the cylindrical heat source solution. *ASHRAE Transaction: Research* 3472, 287-295.

Gao, J., X. Zhang, J. Liu, K.S. Li and J. Yang 2008. Thermal performance and ground temperature of vertical pile-foundation heat exchangers: A case study. *Applied Thermal Engineering* 28(17), 2295-2304.

Hamada, Y., H. Saitoh, M. Nakamura, H. Kubota and K. Ochifuji 2007. Field performance of an energy pile system for space heating. *Energy and Buildings* 39(5), 517-524.

Jun, L., Z. Xu, G. Jun and Y. Jie 2009. Evaluation of heat exchange rate of GHE in geothermal heat pump systems. *Renewable Energy* 34(12), 2898-2904.

Lamarche, L. and B. Beauchamp 2007. A new contribution to the finite line-source model for geothermal boreholes. *Energy and Buildings* 39(2), 188-198.

Marcotte, D. and P. Pasquier 2008. Fast fluid and ground temperature computation for geothermal ground-loop heat exchanger systems. *Geothermics* 37(6), 651-665.

Miyara, A., K. Tsubaki, S. Inoue and K. Yoshida 2011. Experimental study of several types of ground heat exchanger using a steel pile foundation. *Renewable Energy* 36(2), 764-771.